Evidence for excited spin-orbit state reaction dynamics in $F+H_2$: Theory and experiment

François Lique,[1] Millard H. Alexander,[1,a)] Guoliang Li,[2,b)] Hans-Joachim Werner,[2,c)] Sergey A. Nizkorodov,[3,d)] Warren W. Harper,[3] and David J. Nesbitt[3,e)]
[1]*Department of Chemistry and Biochemistry and Institute for Physical Science and Technology, University of Maryland, College Park, Maryland, 20742-2021, USA*
[2]*Institüt für Theoretische Chemie, Universität Stuttgart, Pfaffenwaldring 55, D-70569 Stuttgart, Germany*
[3]*JIlA, University of Colorado and National Institute of Standards and Technology and Department of Chemistry and Biochemistry, University of Colorado, Boulder, Colorado 80309-0440, USA*

(Received 22 October 2007; accepted 12 December 2007; published online 29 February 2008)

We describe fully quantum, time-independent scattering calculations of the $F+H_2 \rightarrow HF+H$ reaction, concentrating on the HF product rotational distributions in $v'=3$. The calculations involved two new sets of *ab initio* potential energy surfaces, based on large basis set, multireference configuration-interaction calculations, which are further scaled to reproduce the experimental exoergicity of the reaction. In addition, the spin-orbit, Coriolis, and electrostatic couplings between the three quasidiabatic $F+H_2$ electronic states are included. The calculated integral cross sections are compared with the results of molecular beam experiments. At low collision energies, a significant fraction of the reaction is due to Born–Oppenheimer forbidden, but energetically allowed reaction of F in its excited ($^2P_{1/2}$) spin-orbit state. As the collision energy increases, the Born–Oppenheimer allowed reaction of F in its ground ($^2P_{3/2}$) spin-orbit state rapidly dominates. Overall, the calculations agree reasonably well with the experiment, although there remains some disagreement with respect to the degree of rotational excitation of the HF($v'=3$) products as well as with the energy dependence of the reactive cross sections at the lowest collision energies. © *2008 American Institute of Physics*. [DOI: 10.1063/1.2831412]

I. INTRODUCTION

Because of its experimental accessibility, the reaction of F with H_2 and its isotopomers has become the paradigm for exothermic triatomic reactions. The appearance, in 1996, of the high-quality *ab initio* potential energy surface (PES) of Stark and Werner[1] (SW) has led to a number of quantum-scattering investigations, as well as quasiclassical trajectory studies of this reaction.[2,3] This theoretical work has successfully reproduced the major features seen in molecular-beam scattering studies of the reaction of F with H_2, D_2, and HD.

The approach of the H_2 molecule splits the degeneracy of the ^2P state of the F atom. As shown schematically in Fig. 1, reaction to yield HF in its electronic ground state occurs only on the lowest electronic state ($1\,^2A'$; $^2\Sigma^+$ in linear geometry). Two other electronic states ($2\,^2A'$ and $1\,^2A''$; $^2\Pi$ in linear geometry) correlate adiabatically with electronically excited states of the products [HF($a\,^3\Pi$)+H(^2S)] which are energetically inaccessible at low to moderate collision energies. If the reaction were to proceed adiabatically, then the spin-orbit excited F atom ($^2P_{1/2}$), which lies 404 cm^{-1} (1.15 kcal/mol) above the ground state, would not react. We further see in Fig. 1 that the potential energy surface which correlates in the asymptotic region of the reactant arrangement with the spin-orbit excited F atom does not correlate with ground-state HF products. Consequently, within the Born–Oppenheimer approximation, reaction of the spin-orbit excited F atom is forbidden.[4,5]

Earlier scattering studies indicate that the reactivity of the excited spin-orbit state is below the sensitivity level of these experiments at collision energies below 2 kcal/mol. (As listed in Table I, the barrier to reaction with the full spin-orbit Hamiltonian included, but uncorrected for zero-point effects, is ≈1.5 kcal/mol.[6]) In molecular-beam experiments on the F+HD reaction, Dong *et al.* also found that the reactivity of the spin-orbit excited state was only a few percent of that of the ground state.[7] Just this year, Che *et al.* have presented a high-resolution molecular-beam study of the $F+D_2$ reaction at collision energies down to 0.2 kcal/mol.[8] They report that the relative reactivity of the F* atom increases steadily from ≈0.25 at a collision energy of 1.1 kcal/mol up to ≈1.5 as the collision energy decreases to 0.25 kcal/mol.

Theoretical investigations of the reactivity of the F* atom date back a quarter century.[9] To investigate this correctly, one needs three potential energy surfaces as well as an accurate description of the couplings (nonadiabatic, spin-

a)Electronic mail: mha@umd.edu. URL: www.chem.umd.edu/groups/alexander.
b)Present address: School of Chemistry and Environment, South China Normal University, Guangzhou, Guangdong, 510006, People's Republic of China. Electronic mail: glli77@yahoo.com.cn.
c)Electronic mail: werner@theochem.uni-stuttgart.de. URL: www.theochem.uni-stuttgart.de.
d)Present address: Department of Chemistry, University of California, Irvine, California 92697-2025. Electronic mail: nizkorod@uci.edu.
e)Electronic mail: djn@jila.colorado.edu. URL: http://www.colorado.edu/Chemistry/people/nesbittd.html.

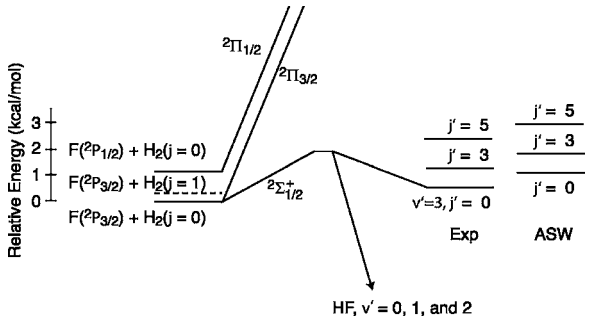

FIG. 1. Schematic plot of the energetics of the $F+H_2 \rightarrow HF+(v'=3)+H$ reaction. The relative reactant energies, the position of the barrier and the position of the indicated HF channels are drawn to scale. The dashed line indicates the position of the lowest ($j=1$) level of oH_2. The right hand side shows the position of three of the HF($v'=3,j'$) product levels. As is shown, the 0.619 kcal/mol error in the $v'=3$ exoergicity predicted by the ASW potential energy surfaces (see text) results in a substantial displacement in the predicted positions of these product levels. The errors in the $v'=3$ exoergicities for the LWA-78 and LWA-5 potential energy surfaces are, respectively, 0.002 and 0.127 kcal/mol.

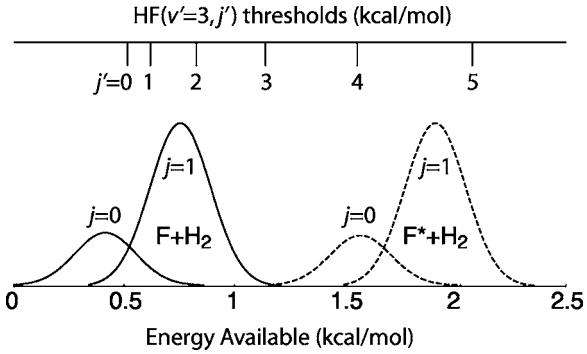

FIG. 2. Schematic view of the available energy for the reaction of F($^2P_{3/2}$) and F*($^2P_{1/2}$) at a collision energy of 0.415 kcal/mol. The Gaussian functions indicate the distribution of translational energies at this nominal collision energy in the experiments of Nesbitt and co-workers (FWHM =0.162 kcal/mol). The solid curves illustrate the distribution of translational energies for reaction of F($^2P_{3/2}$) with, respectively, H_2 in rotational levels $j=0$, 1, and 2. The dashed curves illustrate the distribution of translational energies for reaction of F*($^2P_{1/2}$) with H_2 in rotational levels $j=0$ and 1. The heights of the Gaussian distributions correspond to the relative weights of the $j=0$ and 1 rotational levels in n-H_2 at $T=200$ K. Across the top appear the threshold energies for production of HF($v'=3,j'$) for $j'=0-5$. As can be seen, if just the $j=0$ and 1 levels of H_2 are populated, then HF rotational levels with $j'>3$ can be produced only by reaction of the spin-orbit excited atom.

orbit, and Coriolis) between them. In several recent papers, we presented the framework for the accurate investigation of the reactivity of the F* atom, based an *ab initio* description which includes all three PESs and the necessary couplings and with a subsequent fully quantum treatment of the scattering.[10–12] These recent advancements overcome the approximations which have characterized earlier, multiple potential surface studies of the $F+H_2$ reaction. Our framework has been used subsequently by Han and co-workers in time-dependent studies which retain the crucial spin-orbit coupling between the three PESs but neglect the less-important nonadiabatic and Coriolis couplings.[13–16]

In our earlier work, we found the reactivity of the excited ($^2P_{1/2}$) spin-orbit state of F to be at most 25% of that of the ground spin-orbit state.[11,17,18] Because of the greater statistical weight of the ground spin-orbit state (2:1), in most experiments, the effective contribution of the excited spin-orbit state will be reduced by an additional factor of 2. For a given HF product state, the additional energy of the excited spin-orbit state (404 cm^{-1}) of the F atom reactant will manifest itself in a slightly higher translational energy of the HF product. With a sufficiently high degree of energy resolution, these slightly fast HF products can be seen in time-of-flight spectra, as has been reported by Dong *et al.* [for F+HD $\rightarrow$FH+D, (Ref. 7)] and Che *et al.* [for $F+D_2 \rightarrow FD+D$ (Ref. 8)]. Alternatively, at sufficiently low collision energy, the excited spin-orbit reactant will allow formation of HF products in high vibration-rotation levels, which will be energetically inaccessible for reaction of the ground-state F atom. This selectivity underlies the recent experiments of Nesbitt and co-workers.[19–21] As seen schematically in Fig. 2, the higher rotational levels of HF($v'=3$) are energetically inaccessible in reactions of H_2 ($v=0$, $j=0$ and 1) with F in the ground spin-orbit state. Consequently, at low collision energy, these product states can be formed only by reaction of the spin-orbit excited atom.

TABLE I. Calculated and experimental energetics (kcal/mol) for the F($^2P_{3/2}$)+H_2 reaction.

	E_a[a]	ΔE_{00}[b]	ΔE_{03}[c]
ASW	1.93	−31.34	1.134[d]
LWA-5	1.64	−31.90	0.642[d]
LWA-78	1.49	−32.01	0.517[d]
CCSDTQ/CBS[e]	1.63	−32.008	⋯
Expt.	⋯	−32.001(14)[f]	0.515(14)[d]

[a]Abstraction barrier height.
[b]Zero-point-corrected reaction exoergicity for formation of HF($v'=0$).
[c]Zero-point-corrected reaction exoergicity for formation of HF($v'=3$).
[d]ΔE_{00} plus the difference between the calculated or experimental $v=3$ and $v=0$ HF band origins.
[e]Coupled-cluster calculations with inclusion of single, double, triple, and quadruple excitations and extrapolated to the complete basis set limit (see Table V of Ref. 29).
[f]Reference 20.

A direct theoretical comparison with the experiments of Nesbitt and co-workers has been, hitherto, challenging. The Alexander–Stark–Werner (ASW) potential energy surface predicts an exoergicity for the $F(^2P_{3/2})+H_2 \rightarrow HF+H$ reaction which is $\approx$0.7 kcal/mol *too low* (see Table I). Consequently, the endoergicity of the reaction to produce HF($v'=3$) is increased from 0.5 to 1.1 kcal/mol. Because this error is comparable to the spin-orbit splitting in the F atom (1.15 kcal/mol) and, also, to the relative translational energy in the experiments of Nesbitt and co-workers (0.3–2 kcal/mol), it is difficult to use scattering calculations based on the ASW potential energy surfaces to simulate quantitatively the experiments of Nesbitt and co-workers with an energy resolution high enough to allow a precise comparison. As Tzeng and Alexander have discussed,[18] the most meaningful comparison involves an *ad hoc* shift in the collision energy in the theoretical simulations. However, this arbitrary shift confuses any comparison with experiment.

Subsequent to the work of Stark and Werner,[1] there have appeared several more recent *ab initio* investigations, which result in improved estimates of the $F+H_2 \rightarrow HF+H$

exoergicity.[22–24] Unfortunately, these studies have been limited to the lowest potential energy surface, and hence cannot be used to model the spin-orbit dependence of the reaction cross sections. Recently, however, we have described new *ab initio* FH_2 potential energy surfaces.[6] By the use of a very large atomic orbital basis set and by, in addition, scaling the external correlation energy,[25] we were able to obtain virtually exact agreement with the experimental exoergicity, and, in particular for the endoergicity of the $HF(v'=3)$ channel. In this article, we attempt, using full quantum-scattering calculations based on these new PESs, to determine the magnitude of the contribution of spin-orbit-excited F to the cross sections for production of HF in $v'=3$. In addition, the calculated cross sections will be compared with as yet unpublished experimental results, which extend those presented earlier,[19,20] and which reveal the energy dependence of the reactive cross sections for formation of individual rotational levels of the HF products in $v'=3$.

The organization of this paper is as follows: First, Secs. II–IV contain a brief review of the potential energy surfaces used and the treatment of the dynamics. Section V then contains a description of the high-resolution infrared absorption technique used to probe the HF products. Section VI presents the results, both of the simulations and of the experiment. A brief discussion concludes.

II. POTENTIAL ENERGY SURFACES AND SCATTERING CALCULATIONS

As discussed in our earlier publications,[11,26] a full description of the $F+H_2$ reaction requires three potential energy surfaces, two corresponding to electronic states of $^2A'$ symmetry in C_s geometry and the third to a state of $^2A''$ symmetry. In addition, in a quasidiabatic framework, there is a fourth potential energy surface which describes the coupling between the two states of $^2A'$ symmetry. In our previous application of this formalism, we used the set of diabatic potential energy surfaces—designated the ASW potential energy surfaces—based on an extension of the original work of Stark and Werner.[1] As mentioned earlier, a major drawback of these potential energy surfaces is that the exoergicity for the $F+H_2 \rightarrow HF+H$ reaction is predicted to be ≈ 0.66 kcal/mol too small.

Recently, we have presented the results of new *ab initio* calculations,[6] in which both the atomic orbital basis set and multiconfiguration active space were larger than in the calculations of Stark and Werner.[1] In addition, by scaling the external correlation energy by a factor greater than unity, we were able to reproduce the $v'=3$ exoergicity to within 0.01 kcal/mol. The set of potential energy surfaces corresponding to our more recent work is denoted Li–Werner–Alexander (LWA-78), where the number indicates that the external correlation energy was scaled by a factor of 1.078. With a slightly smaller scaling factor ($s=1.05$), the exoergicity is 0.1 kcal too low, however, the resulting potential energy surface, designated LWA-5, reproduces, almost quantitatively, the energy dependence of the transition state resonance observed by Liu and co-workers in the $F+HD \rightarrow FH+D$ reaction.[27,28] Table I summarizes the barrier heights and exoergicities predicted by the ASW, LWA-78, and LWA-5 potential energy surfaces and compares these with experiment and the results of recent benchmark coupled-cluster calculations by Werner–Kállay–Gauss (WKG),[29] which included, exactly, all single, double, triple, and quadruple excitations from the original reference determinant with an additional extrapolation to the complete basis set limit. As can be seen, the barrier height on the LWA-5 surface is in nearly perfect agreement with the predictions of WKG, while the LWA-78 barrier is 0.15 kcal/mol too small. However, the exoergicity on the LWA-78 PES is virtually identical to both the predictions of WKG and to the experimental value, while the LWA-5 exoergicity is 0.1 kcal/mol too small.

We used the time-independent treatment of the reactive scattering described earlier.[11] Calculations were carried out for the ASW, LWA-78, and LWA-5 sets of FH_2 potential energy surfaces, using our extensively modified version[11] of the ABC code of Skouteris *et al.*[30] Here, in contrast to the previous paper of Tzeng and Alexander,[18] no energy shift was applied to the ASW calculations. Additionally, we carried out scattering calculations using just the lowest fully adiabatic FH_2 potential energy surface, obtained by diagonalizing, at each geometry, the 6×6 matrix of the interaction potential plus spin-orbit Hamiltonian [the sum of Eqs. (20) and (25) of Ref. 11]. These single-potential-surface calculations were done using the original version of the ABC code.[30]

In a full description of the reaction which, by necessity, includes the spin-orbit states of the F atom, the states in the reactant arrangement are described by the quantum numbers j and k (the rotational angular momentum of the H_2 molecule and its projection along the reactant Jacobi vector), v (the vibrational quantum number of the H_2 molecule), as well as j_a and k_a (the total electronic angular momentum of the F atom and its projection). The value of j_a is either 3/2 or 1/2 for, respectively, the ground and excited spin-orbit states of the F atom. In the product arrangement, the states are described by the quantum numbers j', k', and v' (the rotational, projection, and vibrational quantum numbers of the HF molecule, and σ the projection of the spin of the H atom. The integral cross section for reaction of $F(j_a)$ with $H_2(j,v)$ to give $HF(v',j')$, summed over final state projection quantum numbers and averaged over initial state projection quantum numbers, is given by

$$\sigma_{j_a jv\rightarrow j'v'}(E_{\mathrm{col}}) = \frac{\pi}{k^2_{j,j_a}(2j+1)(2j_a+1)} \sum_{Jk_akk'\eta\sigma'} (2J+1) \times |S^{J\eta}(j_a k_a jkv \rightarrow j'k'v'\sigma'; E_{\mathrm{tot}})|^2. \quad (1)$$

Here, the summation is over all elements of the S matrix between the initial and final states in question, summed over all values of the total angular momentum J (which contribute to the reaction) as well as over both values of the parity ($\eta = \pm 1$). Here also, k_{j,j_a} denotes the initial wavevector. The scattering calculations are carried out on a grid of values of the total energy E_{tot}. The relevant independent variable for the cross sections is, however, the collision energy E_{col}, which is the initial translational energy. The two are related by

$$E_{\mathrm{tot}} = E_{\mathrm{col}} + \varepsilon_{j_a j v}. \tag{2}$$

To compare with an experiment in which the rotational levels of the H_2 reactant are not selected, one must first average the calculated cross sections over the distribution of H_2 rotational levels in the incident beam. We obtain

$$\langle \sigma_{j_a v \to j' v'}(E_{\mathrm{col}}) \rangle_j = \sum_{j=0}^{j_{\max}} w_j \sigma_{j_a j v \to j' v'}(E_{\mathrm{col}}) \Bigg/ \sum_{j=0}^{j_{\max}} w_j, \tag{3}$$

where w_j is the population in rotational level j.

For experiments with n-H_2, as those reported by Nesbitt and co-workers, we assume that in the expansion there is no interconversion of o-H_2 to p-H_2, so that these two isotopomers can be treated as separate species. If we assume that the fractional rotational populations are given by a Boltzmann distribution at temperature T_{rot}, then for even j (p-H_2),

$$w_j = w_{\mathrm{even}} \exp[-j(j+1)B_j/kT_{\mathrm{rot}}], \tag{4}$$

and for odd j (o-H_2),

$$w_j = w_{\mathrm{odd}} \exp\{-[j(j+1)-2]B_j/kT_{\mathrm{rot}}\}. \tag{5}$$

Here, w_{even} and w_{odd} are the nuclear spin statistical weights of the two isotopomers ($w_{\mathrm{even}}=1$ and $w_{\mathrm{odd}}=3$ for n-H_2). The sums over j in Eq. (3) extend, in principle, to infinity; however, for H_2 at rotational temperatures less than 200 K, they may be terminated at $j=2$ without loss of accuracy.

One must then average over the relative populations of the two spin-orbit states of the F atom present in the experiment. We obtain

$$\langle \sigma_{v \to j' v'}(E_{\mathrm{col}}) \rangle_j = f_{3/2} \langle \sigma_{j_a=3/2, v \to j' v'}(E_{\mathrm{col}}) \rangle_j + [1 - f_{3/2}] \times \langle \sigma_{j_a=1/2, v \to j' v'}(E_{\mathrm{col}}) \rangle_j. \tag{6}$$

Here, $f_{3/2}$ is the fraction of the initial F atoms which are in the ground spin-orbit state, namely,

$$f_{3/2} = 2/[2 + \exp(-\Delta E_{\mathrm{so}}/kT_{\mathrm{so}})], \tag{7}$$

where ΔE_{so} is the $^2P_{3/2}-{}^2P_{1/2}$ spin-orbit splitting and T_{so} is the spin-orbit temperature of the F atom source.

In the conventional single-electronic-state description of the F+H_2 reaction the spin-orbit states of the F atom are ignored. Thus, the quantum numbers j_a and k_a do not appear. The expression for the cross section comparable to Eq. (1) is then

$$\sigma_{jv \to j' v'}(E_{\mathrm{col}}) = \frac{\pi}{k_j^2 (2j+1)} \sum_{Jkk'\eta} (2J+1) |S^{J\eta}(jkv \to j' v'; E_{\mathrm{tot}})|^2. \tag{8}$$

This cross section is then averaged over the H_2 rotation, as in Eq. (3). To compare then with the result of a multiple potential energy surface calculation, it is also necessary to multiply by a spin-orbit weighting factor as follows:

$$\langle \sigma_{v \to j' v'}(E_{\mathrm{col}}) \rangle_j = \tfrac{1}{2} f_{3/2} \langle \sigma_{v \to j' v'}(E_{\mathrm{col}})^{1\mathrm{PES}} \rangle_j. \tag{9}$$

The reader should note the additional factor of 1/2 in Eq. (9) when compared to Eq. (6). This reduction arises because of the fundamental difference between the single-PES and multiple-PES descriptions of the reaction.[31] As seen in Fig. 1, four states correlate with the ground state reactants, $F(^2P_{3/2})+H_2$, namely, $\Sigma_{\pm 1/2}$ and $\Pi_{\pm 3/2}$. Of these the Π states are essentially unreactive, so that, in the neglect of nonadiabatic effects, the results of a single-PES calculation must be multiplied by that fraction (50%) of the reactants which approach on the two Σ potential energy surfaces.

A proper comparison with experiment involves the reaction flux R (the product of the cross section and the relative velocity), rather than cross section, and an additional inclusion of the finite width of the translational energy distribution in the experiments described here and in Refs. 19 and 20. Thus we compare, at each nominal value of the experimental collision energy, the average of the calculated fluxes over an assumed Gaussian distribution in the initial collision energy, with full width at half maximum (FWHM) (δE) comparable to the experimental distribution at each nominal collision energy energy E_n. We thus obtain

$$\langle R_{v \to j' v'}(E_n) \rangle = (\alpha/\pi)^{1/2} \int (2E/m)^{1/2} \exp[-\alpha(E-E_n)^2] \times \langle \sigma_{v \to j' v'}(E) \rangle_j dE, \tag{10}$$

where m is the collision reduced mass, $\alpha = 2\ln(1/2)/\delta E$ and the cross section in angle brackets on the right hand side corresponds to Eq. (6) [or Eq. (9)]. Further division by the nominal relative velocity at translational energy E_n gives the following expression for the averaged reaction cross section, which we will compare with experiment:

$$\langle \sigma_{v \to j' v'}(E_n) \rangle = \langle R_{v \to j' v'}(E_n) \rangle / (2E_n/m)^{1/2}. \tag{11}$$

III. EXPERIMENT AND RESULTS

Two sets of experiments were run. Figure 3 shows the values of the nominal collision energies and the associated FWHM of the distributions in collision energy associated with each nominal collision energy.

In the scattering calculations, in each arrangement (F+H_2 or FH+H) all rotational and vibrational levels of the diatomic moiety were included subject to the dual exclusion of (a) levels with internal energy greater than 1.7 eV and (b) levels in which the angular momentum j of the diatomic moiety (either H_2 or HF) is greater than 15. The integration range was divided into 100 sectors spanning a range in the hyperradius ρ extending from 1.5 to 12 bohrs. These integration parameters were sufficient to ensure convergence in the calculated reactive transition probabilities for collision energies up to 3 kcal/mol. For the LWA-5 and LWA-78 sets of potential energy surfaces, calculations were carried out at,

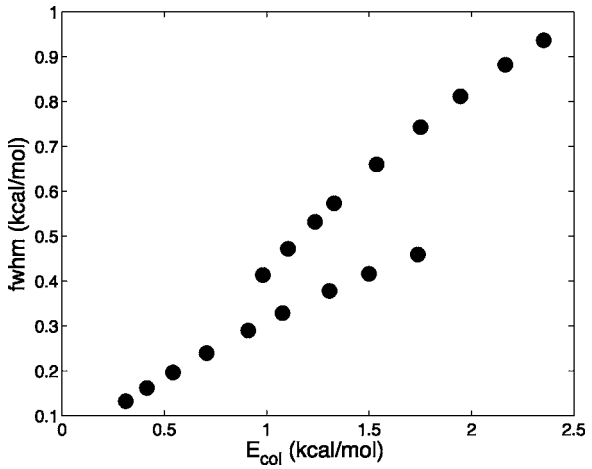

FIG. 3. Full width at half maximum of the collision energy distributions, as a function of the nominal collision energy, in the two sets of experiments.

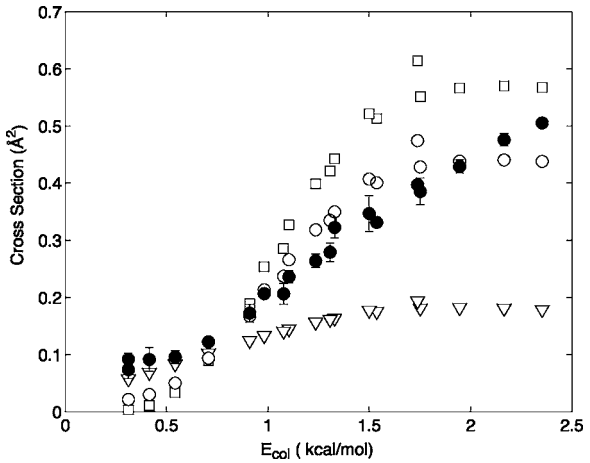

FIG. 4. F+$H_2 \rightarrow$HF($v'=3$)+H averaged reaction cross section [Eq. (12)] as a function of the collision energy, summed over the HF($v'=3$) rotational quantum number, computed on the LWA-78 set of potential energy surfaces. The initial $H_2(v=0,j)$ rotational distribution is 0.243:0.750:0.007 for $j=0$, 1, and 2, respectively. The open squares and open triangles correspond to reaction of the ground ($^2P_{3/2}$) and excited ($^2P_{1/2}$) spin-orbit states of the F atom, while the open circles designate the average over an initial F atom spin-orbit distribution of 2:1 for ($^2P_{3/2}$) and ($^2P_{1/2}$). The experimental data (scaled by 0.37) with associated error bars are depicted by the filled circles.

for reactions with p-H_2, a total of 80 total energies, and, for reactions with o-H_2, a total of 72 total energies. For the calculations based on the ASW set of potential energy surfaces, the energy grid included 53 and 49 energies for reactions with, respectively, p-H_2 and o-H_2. The individual $v,j \rightarrow v',j'$ cross sections were then spline interpolated onto a larger grid of collision energies

For the light H_2 molecule, the higher rotational levels may not be cooled in the expansion as efficiently as the lower levels, so that the reactant rotational distribution may not be described perfectly by a single "temperature." Notwithstanding, for the theoretical simulations presented here the rotational temperature in Eqs. (4) and (5) was taken to be 100 K, and the sum over the H_2 rotational quantum numbers was truncated at $\max(j)=2$. The resulting relative populations of the $j=0$, 1, and 2 levels of H_2 are, respectively, 0.243, 0.750, and 0.007. We also assumed an F*:F population ratio of 1:2 in the discharge source, consistent with a very high spin-orbit temperature.[32]

A. Cross sections summed over final rotational level

The first comparison will be of the reactive cross sections for production of HF in $v'=3$, summed over the HF rotational level, namely,

$$\langle \sigma_{v\rightarrow v'}(E_{\mathrm{col}})\rangle = \sum_{j'} \langle \sigma_{v\rightarrow v'j'}(E_{\mathrm{col}})\rangle_j, \tag{12}$$

where $\langle \sigma_{v\rightarrow v'j'}(E_{\mathrm{col}})\rangle_j$ is given by Eq. (11). This cross section, as a function of collision energy, is presented in Fig. 4 for the results obtained on the LWA-78 potential energy surfaces, and, in Fig. 5 for the results obtained on the LWA-5 and ASW potential energy surfaces. In Fig. 4, we also present the initial-spin-orbit-resolved reactive cross sections determined on the LWA-78 potential energy surfaces, namely, $\langle \sigma_{j_a=3/2v\rightarrow j'v'}(E_{\mathrm{col}})\rangle_j$ and $\langle \sigma_{j_a=1/2v\rightarrow j'v'}(E_{\mathrm{col}})\rangle_j$, again summed over all values of j'. In both cases, we compare the calculated cross sections with the experimental data, discussed above.

Since the absolute magnitude of the cross sections is not determined experimentally, for Figs. 4 and 5, we have scaled the relative experimental cross sections (by 0.37) to obtain good visual agreement with the energy dependence of the calculated cross sections of Eq. (12). We observe, first, that the qualitative dependence on energy of the calculated cross sections is very similar for all sets of potential energy surfaces. The LWA-5 cross sections are slightly smaller in magnitude, most likely because the reaction barrier is slightly higher (Table I).

When we compare Figs. 4 and 5, we observe, as anticipated, that the cross section for the Born–Oppenheimer forbidden (nonadiabatic) reaction of F* is smaller than for the allowed reaction of F. At low collision energies, however,

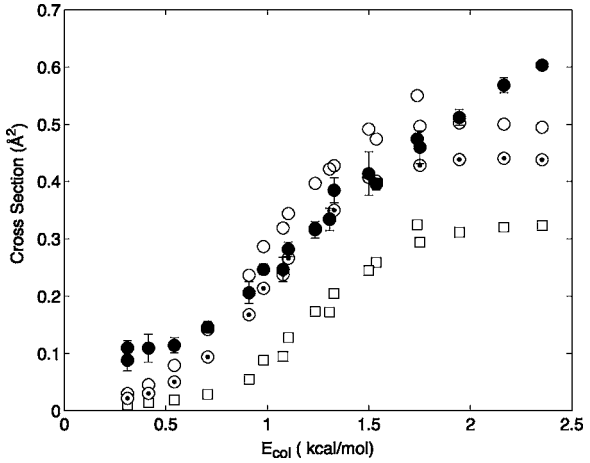

FIG. 5. F+$H_2 \rightarrow$HF($v'=3$)+H averaged reaction cross section [Eq. (12)] as a function of the collision energy, summed over the HF($v'=3$) rotational quantum number, averaged also over an initial F aom spin-orbit distribution of 2:1. The initial $H_2(v=0,j)$ rotational distribution is 0.243:0.750:0.007 for $j=0$, 1, and 2, respectively. The open circles and dotted circles correspond to calculations on the LWA-78 and LWA-5 potential energy surfaces, respectively, and the open squares, to calculations on the ASW potential energy surfaces. The experimental data (scaled by 0.37) and associated error bars are depicted by the filled circles.

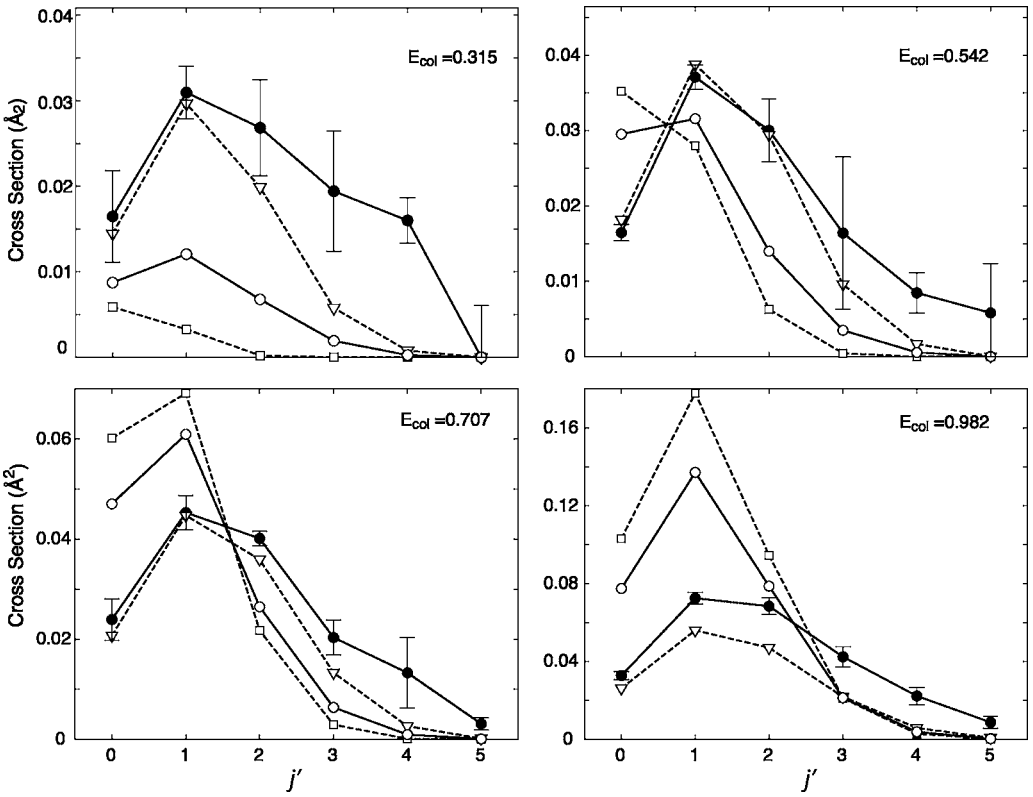

FIG. 6. $F+H_2 \rightarrow HF(v'=3,j')+H$ averaged reaction cross section [Eq. (12)] as a function of the HF rotational quantum number at four collision energies (kcal/mol), computed for the LWA-78 set of potential energy surfaces. The initial $H_2(v=0,j)$ rotational distribution is 0.243:0.750:0.007 for $j=0$, 1, and 2, respectively. The open squares and open triangles correspond to reaction of the ground ($^2P_{3/2}$) and excited ($^2P_{1/2}$) spin-orbit states of the F atom, while the open circles designate the average over an initial F atom spin-orbit distribution of 2:1 for ($^2P_{3/2}$) and ($^2P_{1/2}$). The experimental data, with associated error bars, is depicted by the filled circles. The sum of both the experimental and the theoretical equals the values shown in Fig. 4.

where reaction of F is energetically constrained (see Fig. 2), the nonadiabatic pathway becomes dominant. It is this crossover, seen clearly in Figs. 4 and 5 which is responsible for the slow decrease in the experimental cross sections at the lowest collision energies, as suggested several years ago by Nizkorodov *et al.*[20] Notwithstanding, when we average the cross section for the $F+H_2$ and F^*+H_2 reactions, weighted by the 2:1 F:F* statistical ratio, we see, as shown in the lower panels of Figs. 4 and 5, that the calculated cross sections do drop off somewhat faster at low collision energy than the experimental values. Overall, though, the agreement with experiment is reasonably good, and, in particular, noticeably improved when compared to the predictions of the ASW set of potential energy surfaces, as shown in Fig. 5. Additionally, the theoretical predictions shown in Figs. 4 and 5 agree significantly better with experiment than earlier predictions[20] based on the SW PES (not shown here).

B. Final-*j* resolved cross sections

As suggested by Figs. 1 and 2, a more sensitive probe of the relative reactivity will be the examination of the dependence on the HF final rotational quantum number of the reactive cross section for formation of $HF(v'=3)$. Here, at low collision energy, only reaction of the excited spin-orbit state can lead to production of the higher ($j'=3$, 4, and 5) rotational levels. Figure 6 displays this j' dependence for $E_{col}=0.311$, 0.542, 0.707, and 0.982 kcal/mol, and compares the theoretical predictions with the experimental results. The calculations pertain to the LWA-78 set of potential energy surfaces. We prefer here to use the single scaling factor of 0.37 (see above) for the comparison at all energies, rather than separately (and arbitrarily) scaling the experimental data at each collision energy.

We observe in Fig. 6 that at the low collision energy of 0.315 kcal/mol, reaction of the excited spin-orbit state makes the major contribution to the reactive cross section. The overall dependence on j' of the calculated cross sections, when averaged over an assumed 2:1 ratio of F to F*, agrees quite well with the experiment, except that the experimental cross sections are larger at this collision energy (see Fig. 4). At $E_{col}=0.542$ kcal/mol, the conclusions are similar, except that the theoretical simulations tend to underestimate the degree of rotational excitation seen in the experiment.

At higher collision energy the contribution of the adiabatically allowed reaction of F, as opposed to the reaction of F*, becomes increasingly important. However, the underestimation of the degree of rotational excitation predicted by the experiment remains true at the higher collision energies considered. In fact, calculations based on the ASW, LWA-5, and LWA-78 sets of potential energy surfaces all predict, uniformly, a significantly lower degree of rotational excitation than seen experimentally. This is shown clearly in Fig. 7 which plots the average value of the rotational excitation in $HF(v'=3)$, defined by

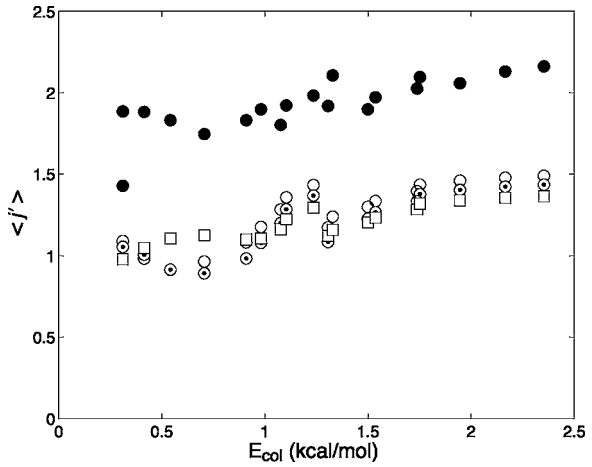

FIG. 7. Average rotational excitation of HF products in the $v'=3$ vibrational manifold as a function of the nominal collision energy, [see Eq. (13)]. The filled circles indicate the experimental results, while the open circles and dotted circles correspond to calculations on the LWA-78 and LWA-5 potential energy surfaces, respectively, and the open squares to calculations on the ASW potential energy surfaces.

$$\langle j'(E_{\mathrm{col}})\rangle = \sum_{j'} j' \langle \sigma_{v\to v'j'}(E_{\mathrm{col}})\rangle_j \Big/ \sum_{j'} \langle \sigma_{v\to v'j'}(E_{\mathrm{col}})\rangle_j. \tag{13}$$

The scatter in the values of $\langle j'\rangle$ reflects the varying widths of the experimental collision energy distributions for different nominal values of the collision energy (see Fig. 3). We observe that all three sets of potential energy surfaces (ASW, LWA-5, and LWA-78) predict virtually the same degree of rotational excitation, which is substantially less than that found experimentally.

C. Comparison of single and multiple potential energy surface simulations

The vast majority of prior theoretical investigations of the F+H_2 reactions, whether classical or quantum, have assumed the reaction can be described accurately by calculations based on a single potential energy surface, thereby ignoring the two repulsive F+H_2 potential energy surfaces (see Fig. 1), as well as nonadiabatic transitions between trajectories evolving on the three potential energy surfaces. As discussed above, we can evaluate the accuracy of this approximation by calculations in which only the lowest electronically adiabatic potential energy surfaces is retained, and in which the open-shell character of the F atom is ignored. This comparison is shown in Fig. 8. We see that at the lowest of the three collision energies ($E_{\mathrm{col}}=0.311$ kcal/mol), the cross sections predicted by the single-potential-surface calculations lie substantially below the multiple-surface results. At this collision energy, the F* reaction, which is not included in the single-surface calculations, makes a substantial contribution, particularly at the higher values of j', where the reaction of the ground spin-orbit state is increasingly endoergic (Fig. 2). As the collision energy increases, though, the single- and multiple-surface cross sections agree increasingly better, because the contribution of the F* channel becomes less important.

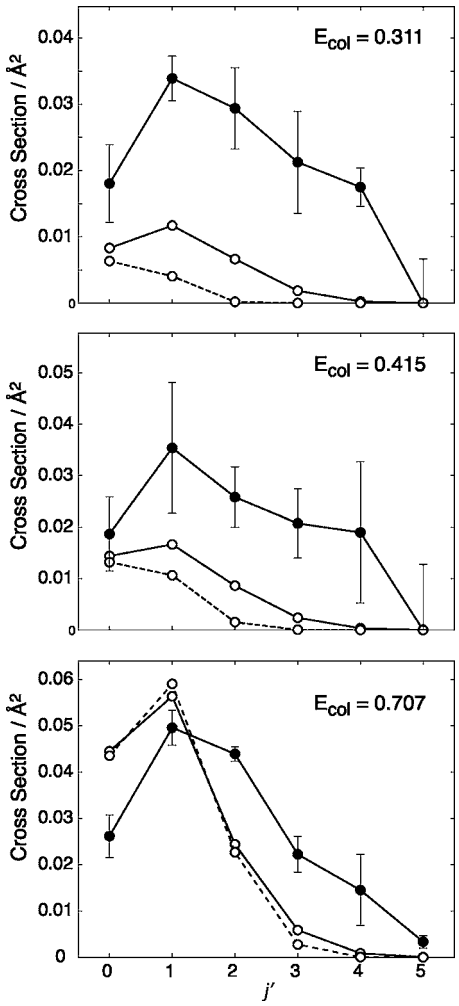

FIG. 8. F+$H_2\rightarrow$HF($v'=3,j'$)+H averaged reaction cross section [Eq. (12)] as a function of the HF rotational quantum number at collision energies of 0.311, 0.415, and 0.707 kcal/mol, computed for the LWA-78 set of potential energy surfaces. The initial $H_2(v=0,j)$ rotational distribution is 0.243:0.750:0.007 for $j=0$, 1, and 2, respectively. The open circles and solid line correspond to the average of the F and F* cross sections; under the assumption of an initial F atom spin-orbit population of 2:1 for ($^2P_{3/2}$) and ($^2P_{1/2}$). The open circles and dashed line correspond to the result of a single potential energy surface calculation using the lowest fully adiabatic LWA-78 potential energy surface [see Eq. (9)]. The experimental data, with associated error bars, are depicted by the filled circles and has been scaled identically to Fig. 4.

IV. DISCUSSION AND CONCLUSION

We have presented here a comparison between final-state-resolved experimental studies of the F+$H_2\rightarrow$HF($v'=3$)+H reaction and quantum reactive scattering calculations based on fits to accurate *ab initio* potential energy surfaces obtained using highly correlated, multireference configuration-interaction wavefunctions. The full open-shell character of the F atom was included explicitly. The comparison shows that at low collision energies, where the HF($v'=3$) vibrational manifold, especially the higher rotational levels, is energetically inaccessible for reaction with F in its ground ($^2P_{3/2}$) spin-orbit state, a significant fraction of the reaction is due to Born–Oppenheimer forbidden, but energetically allowed, reaction of F in its excited ($^2P_{1/2}$) spin-orbit state. As the collision energy increases, the Born–Oppenheimer allowed reaction of F in its ground ($^2P_{3/2}$)

spin-orbit state rapidly dominates. The experimentally determined cross sections, both summed over final rotational state as well as rotationally state resolved, agree well with the calculations, particularly with those on the recent Li–Werner–Alexander (LWA-78) potential energy surface, which are based on *ab initio* calculations in which the external correlation energy is scaled so that the calculated exoergicities are correct.

At a finer level of comparison, however, there are two significant differences between the simulations and the experiment. First, at very low collision energies, the calculated cross sections for formation of $HF(v'=3)$, even including the nonadiabatic F^*+H_2 channel, drop to zero, while the experiment shows a levelling off. Second, at all collision energies investigated, experiment shows a larger degree of rotational excitation of the $HF(v'=3)$ products than predicted by the scattering calculations. Unfortunately, these differences between the predictions of our quantum scattering calculations and the results of experiment remain unchanged for three sets of potential energy surfaces, based both on the newer *ab initio* calculations of Li and Werner[6] and on the older calculations of Stark and Werner[1].

It is possible that these differences reflect some fundamental inaccuracies in either the important nonadiabatic couplings or in the dependence on geometry of all three of these potential energy surfaces, particularly in the product arrangement, where the HF and H fragments are separating and where the resultant torques on the HF fragment result give rise to the HF rotational distribution in each vibrational manifold. However, recent calculations on the $F+D_2$ reaction based on the LWA-78 potential energy surface reveal an exceptionally good agreement with the molecular beam experiments of Che *et al.*,[8] both for the relative F^*/F reactivity as a function of collision energy and for the subtle details of the final state resolved differential cross sections. This agreement argues in favor of the accuracy of both the LWA-78 potential energy surfaces and our treatment of the reactive collision dynamics. Alternatively, it is possible that the distribution of collision velocities in the experiment is more complex than the simple Gaussian function assumed in Eq. (10).

Another possible explanation of the discrepancy between theory and experiment is that the rotational cooling of the H_2 reactant is incomplete, so that the fractional population in $j=2$ is higher than that given by a Boltzmann distribution at $T=100$ K. However, simulations with a rotational temperature of 200 K, which increases the fractional population in $j=2$ tenfold (from 0.007 to 0.071), lead to a barely visible shift in the rotational distributions at $E_c=0.311$ kcal/mol (upper left panel in Fig. 6), far less than the difference between theory and experiment.

There have appeared recently several new calculations of potential energy surfaces for the FH_2 system.[22–24] These, however, have been limited to the lowest $^2A'$ potential energy surface, so cannot be used directly in a study of nonadiabaticity in the $F+H_2$ reaction. However, in the product arrangement, only the lowest potential energy surface correlates with HF+H products in their electronic ground state (Fig. 1), so that, possibly, the $HF(v'=3)$ rotational distributions predicted by calculations on these other potential energy surfaces could be used to challenge or confirm the rotational distributions predicted by the scattering calculations reported here.

One limitation in the investigation of the $F+H_2$ reaction is that if n-H_2 is used, then even after expansion through a supersonic nozzle, ≈75% of the initial beam remains in the $j=1$ rotational level. As seen in Fig. 2, since the rotational energy in $H_2(v=0,j=1)$ is ≈30% of the spin-orbit splitting in the F atom, the presence of this rotationally excited reactant blurs the comparison of Born–Oppenheimer-allowed and Born–Oppenheimer-forbidden mechanisms at low energy. This freezing out of the reactant rotational distribution can be avoided by using HD instead of H_2. Indeed, Harper *et al.* have presented a similar study of the F+HD reaction[21], in which, as in the present study, investigation of $HF(v'=3)$ products shows clear evidence of the importance of the Born–Oppenheimer forbidden process at low collision energy. Because of the loss of the diatomic reflection symmetry, when replacing H_2 by HD, the multiple potential energy surface scattering calculations are more computationally intensive for the F+HD reaction. These calculations are now in progress and will be reported soon.

In summary, the full multiple potential energy surface calculations indicate an improved degree of agreement with experiment, although the discrepancies still exceed the experimental uncertainties. The good overall agreement confirms our basic conclusion, which goes back to our earlier work,[11] that cross sections for the Born–Oppenheimer-forbidden reaction of F* with molecular hydrogen is a relatively small fraction of those for the corresponding Born–Oppenheimer-allowed reaction of F. However, this predominance of the F channel is greatly diminished at low collision energies by threshold effects, in particular, where the additional spin-orbit energy renders specific $HF(v=3,j')$ levels allowed. However, in the case of the similar $Cl+H_2$ reaction, there is little agreement between theory[4] and experiment[33,34] as to the importance of the Born–Oppenheimer-forbidden pathway, a situation which is still not understood.

ACKNOWLEDGMENTS

M.H.A is grateful to the U.S. National Science Foundation for support under Grant No. CHE-0413743. H.J.W acknowledges generous support from the Deutsche Forschungsgemeinschaft (Leibniz program) and the Fonds der Chemischen Industrie. D.J.N would like to acknowledge funding from the Air Force Office of Scientific Research, as well as additional support from the U.S. National Science Foundation in the development of the discharge radical sources.

[1] K. Stark and H.-J. Werner, J. Chem. Phys. **104**, 6515 (1996).
[2] D. E. Manolopoulos, J. Chem. Soc., Faraday Trans. **93**, 673 (1997).
[3] S. C. Althorpe and D. C. Clary, Annu. Rev. Phys. Chem. **54**, 493 (2003).
[4] M. H. Alexander, G. Capecchi, and H.-J. Werner, Science **296**, 715 (2002).
[5] D. E. Manolopoulos, Science **296**, 664 (2002).
[6] M. H. Alexander, F. Lique, G. Li, and H.-J. Werner, J. Chem. Phys. **127**, 174302 (2007).

[7] F. Dong, S.-H. Lee, and K. Liu, J. Chem. Phys. **113**, 3633 (2000).
[8] L. Che, Z. Ren, X. Wang, W. Dong, D. Dai, X. Wang, D. H. Zhang, X. Yang, G. Li, H.-J. Werner, F. Lique, and M. H. Alexander, Science **317**, 1061 (2007).
[9] J. C. Tully, J. Chem. Phys. **60**, 3042 (1974).
[10] M. H. Alexander, H.-J. Werner, and D. E. Manolopoulos, J. Chem. Phys. **109**, 5710 (1998).
[11] M. H. Alexander, D. E. Manolopoulos, and H.-J. Werner, J. Chem. Phys. **113**, 11084 (2000).
[12] M. H. Alexander, Y.-R. Tzeng, and D. Skouteris, in *Chemical Reaction Dynamics*, edited by A. Laganá and G. Lendvay (Kluwer Academic, Amsterdam, 2004), pp. 45–65.
[13] T. X. Xie, Y. Zhang, M. Y. Zhao, and K. L. Han, Phys. Chem. Chem. Phys. **5**, 2034 (2003).
[14] Y. Zhang, T. X. Xie, K. L. Han, and J. Z. H. Zhang, J. Chem. Phys. **119**, 12921 (2003).
[15] T. S. Chu, Y. Zhang, and K. L. Han, Int. Rev. Phys. Chem. **25**, 201 (2006).
[16] Y. Zhang, T. X. Xie, K. L. Han, and J. Z. H. Zhang, J. Chem. Phys. **124**, 134301 (2006).
[17] Y.-R. Tzeng and M. H. Alexander, J. Chem. Phys. **121**, 5812 (2004).
[18] Y.-R. Tzeng and M. H. Alexander, Phys. Chem. Chem. Phys. **6**, 5018 (2004).
[19] W. B. Chapman, B. W. Blackmon, and D. J. Nesbitt, J. Chem. Phys. **107**, 8193 (1997).
[20] S. A. Nizkorodov, W. W. Harper, and D. J. Nesbitt, Faraday Discuss. Chem. Soc. **113**, 107 (1999).
[21] W. W. Harper, S. A. Nizkorodov, and D. J. Nesbitt, J. Chem. Phys. **116**, 5622 (2002).
[22] M. Hayes, M. Gustafsson, A. M. Mebel, and R. T. Skodje, Chem. Phys. **308**, 259 (2004).
[23] W. Cardoen, R. Gdanitz, and J. Simons, J. Phys. Chem. A **110**, 564 (2006).
[24] C. X. Xu, D. Q. Xie, and D. H. Zhang, Chin. J. Chem. Phys. **19**, 96 (2006).
[25] F. B. Brown and D. G. Truhlar, Chem. Phys. Lett. **117**, 307 (1985).
[26] M. H. Alexander, G. Capecchi, and H.-J. Werner, Faraday Discuss. Chem. Soc. **127**, 59 (2004).
[27] R. T. Skodje, D. Skouteris, D. E. Manolopoulos, S.-H. Lee, F. Dong, and K. Liu, J. Chem. Phys. **112**, 4536 (2000).
[28] K. Liu, R. T. Skodje, and D. E. Manolopoulos, PhysChemComm **4**, 27 (2002).
[29] H.-J. Werner, M. Kállay, and J. Gauss, J. Chem. Phys. **128**, 034305 (2008).
[30] D. Skouteris, J. F. Castillo, and D. E. Manolopoulos, Comput. Phys. Commun. **133**, 128 (2000).
[31] F. J. Aoiz, L. Bañares, and J. F. Castillo, J. Chem. Phys. **111**, 4013 (1999).
[32] M. Alagia, V. Aquilanti, D. Ascenzi, N. Balucani, D. Cappelletti, L. Cartechini, P. Casavecchia, F. Pirani, G. Sanchini, and G. G. Volpi, Isr. J. Chem. **37**, 329 (1997).
[33] S.-H. Lee, L.-H. Lai, K. Liu, and H. Chang, J. Chem. Phys. **110**, 8229 (1999).
[34] F. Dong, S.-H. Lee, and K. Liu, J. Chem. Phys. **115**, 1197 (2001).